Solubility measurements and modeling of molecules of biological and pharmaceutical interest with supercritical CO_2

G. I. Burgos-Solórzano, J. F. Brennecke* and M. A. Stadtherr

Department of Chemical and Biomolecular Engineering, 182 Fitzpatrick Hall, University of Notre Dame, Notre Dame, IN 46556, USA

Abstract

The tunable nature of the solubility of various compounds, including molecules of pharmaceutical and biological interest, in supercritical fluids (SCFs) makes SCF extraction technology attractive for many separation and purification processes. Exploring new applications requires fundamental understanding of phase behavior. Here we explore the use of supercritical CO_2 to dissolve molecules of potential interest to the pharmaceutical industry. We present experimental measurements and modeling of the solubility of caffeine, uracil and erythromycin in supercritical CO_2 at temperatures between 40 and 60 °C and pressures up to 300 bar. The solubilities are between 10^{-6} and 10^{-3} mole fraction. The solubility behavior is modeled with the Peng-Robinson equation of state (EOS), which correlates the experimental solubility data of caffeine and uracil quite accurately. However, for erythromycin larger deviations are found. Different property estimation techniques are investigated and their influence on the ability to correlate the data with the Peng-Robinson EOS is explored. The combination of computational and experimental tools used here allows the verification of the integrity of

* Corresponding author. Tel.:+1-574-6315847; fax:+1-574-6318366. E-mail address: jfb@nd.edu

the experimental technique and the evaluation of supercritical fluid extraction as an alternative method of purification.

Keywords: Caffeine (xanthine); Uracil (nucleoside); Erythromycin (antibiotic); Solid-fluid equilibria; Supercritical; Equation of state.

1. Background

Exploitation of supercritical fluid extraction (SFE) for industrial applications has taken advantage of the tunable solvating nature of SCFs and the potential fundamental improvements that this technology provides for the purification of products over traditional processes. For example, in the food and pharmaceutical industries, where the toxicity of the extraction medium is of concern, CO_2, the most widely used SCF, has been especially useful. In evaluating SFE or SCF antisolvent processes for purification purposes, the phase behavior of the target compounds with CO_2 is of vital importance. Towards this end, numerous experimental and modeling studies have been performed and a broad range of new applications are being developed [1-9]. This includes the recovery of molecules of pharmaceutical and biochemical interest. For instance, Reverchon and Porta [10] proposed supercritical antisolvent precipitation as an alternative to liquid antisolvent precipitation to produce micronized particles of some antibiotics, anti-asthma drugs, biopolymers and other products. Ko et al. [11] and Gordillo et al. [12] measured solubilities of penicillin (antibiotic) in SCFs to verify the viability of SCF technology to reduce the use of organic solvents, the number of steps and, therefore, the expense involved in the separation and purification process (up to 60 steps with other

technologies). Maxwell et al. [13] measured solubilities of antibiotics of veterinarian interest (lasalocid, monensin, narasin and salinomycin) in SC CO_2 in the presence of methanol and water. Macnaughton et al. [6] studied the solubilities of anti-inflammatory drugs. Mehr et al. [14] explored new sources of extraction of caffeine such as guaraná seeds. Other authors [15-17] studied the selective removal (extraction) of theophylline and theobromine (molecules that are stimulants in small quantities) from coffee beans, leaves of tea plants and food products. SC CO_2 is also important in biochemical systems where enzymes are not deactivated by the presence of CO_2. For instance, Wilson and Cooney [18] showed that proteins such as lysozyme and ribonuclease and most free amino acids were unaffected by CO_2 at 300 bar and room temperature so CO_2 could potentially be used in situ in continuous fermentation processes to recover the product.

Although solubility measurements in SC CO_2 are the first key step in evaluating the viability of SFE, thermodynamic modeling can provide feasibility analysis and reduce the number of experimental measurements required [3, 5]. On the other hand, it is important to note that rigorous thermodynamic modeling of solubilities of compounds of biological and pharmaceutical interest can be difficult [6] due to an almost complete lack of knowledge of the physical properties necessary for the pure molecule parameters used in equations of state. A second challenge when modeling solubilities is the stability of the modeled results. As discussed by Xu et al. [19], in addition to the equifugacity condition it is always necessary to verify the stability of the system by tests such as the tangent plane distance criteria and global minimization methodologies.

The molecules studied in this work are important from different prospectives. Extraction of caffeine (Fig. 1a) with SC CO_2 is, no doubt, the most well-known commercial example of SFE technology. Caffeine solubility is used to verify the integrity of the experimental technique by comparison with previous works [15-17, 20, 21]. In addition, modeling results with the Peng-Robinson equation with van der Waals (vdw) mixing rules are presented.

The second molecule, uracil (Fig. 1b), was selected given its importance as a biochemical compound. Uracil is a nitrogenous heterocyclic nucleic-acid base (nucleoside) present in RNA molecules and, therefore, in nucleotides. Its chemistry influences different synthetic pathways as well as enzyme systems and dictates the structure and properties of living cells and organisms. Uracil and other nucleosides are also important for complexation of AMP, dAMP and ε-AMP. Interest in uracil solution chemistry, and solute solubility [22, 23] is growing as the knowledge of its biochemical importance and applications are becoming better known. For instance, Baker et al. [24] used uracil as a model compound to understand the effect of agrochemicals on foliar penetration. Zielenkiewicz et al. [25] studied uracil and its halo and amino derivatives that are of special interest because of their antimetabolic and antitumor properties. Therefore, uracil interactions in aqueous solvents at different temperatures and, in general, its behavior in different media, has become of great interest. Currently, measurements of solubilities of uracil in water and in salt solutions are available in the literature [26-28]; however, we know of no exploration of uracil in supercritical fluids. In this work, we will present experiments and modeling of the solubility of uracil in SC CO_2 at 40 °C and 60 °C.

The third molecule, erythromycin (Fig. 1c), was selected due to its importance as an antibiotic. The SFE of erythromycin might represent a viable alternative because, as with other antibiotics, traditional separation and purification processes are multi-step and expensive. However, there are some reports of a peculiar biological deactivation of erythromycin in the presence of CO_2 [29-31] and this would have to be fully investigated before considering SFE for separation. Erythromycin is used in the treatment of mild to moderate inflammatory acne. Topical products containing erythromycin, a macrolide antibiotic with poor aqueous solubility, are usually formulated as high alcohol content solutions or gels [32]. Erythromycin easily dissolves in most common organic solvents as well as in dilute aqueous acids, where it forms crystalline salts [33]. We are aware of no reports of erythromycin solubility in supercritical fluids. In this work we present experimental measurements and modeling of the solubility of erythromycin in SC CO_2 at 40 °C and 60 °C and between pressures of 150 and 300 bar.

In summary, in this work we present solubility measurements of three molecules (Fig. 1) of pharmaceutical and biochemical importance: caffeine (a xanthine), uracil (a nucleoside) and erythromycin (an antibiotic), in supercritical CO_2. In addition, we model the solubilities with the Peng-Robinson EOS, using van der Waals mixing rules and different parameter estimation techniques. Discussion of the best alternatives for modeling of these compounds is included.

2. Experimental Set-up

2.1 Materials

The sources and purity of materials used in the experiments are as follows: erythromycin, assay ~97% (NT) from Fluka; uracil, ~99% purity, from Sigma; caffeine, anhydrous, from Sigma; water, HPLC grade, from Aldrich; ethanol, 200 proof anhydrous, ~99.5+% purity from Sigma. Carbon dioxide was either supercritical fluid grade from Scott Specialty Gases, Inc. (for measurements with erythromycin and uracil), or high purity grade or bone dry grade from Mittler Supply, Inc. (caffeine measurements).

2.2 Apparatus

Solubility measurements were performed with a custom-built recirculating high pressure apparatus [34], which is shown schematically in Fig. 2. This apparatus is similar in concept to high-pressure recirculating systems that have been used to measure vapor-liquid multiphase equilibrium [35, 36]. The apparatus consists of five main components: pumping, equilibration, heating, sampling and cleaning/venting systems. The *pumping system* consists of an ISCO syringe pump model 260D, which provides the initial pressurization of the equilibration vessel and piping with carbon dioxide. A check valve was placed between the syringe pump and the recirculation system to avoid back flow. The second pump is an Idex, Inc. magnetically driven recirculation pump model 1805R-415A, whose function is to take the solute/CO_2 mixture from the equilibration vessel, pass it through the sample valve and pump it back to the equilibration vessel. A vacuum pump is used for cleaning purposes (see cleaning/venting system). The pressure in the

system was monitored with a digital Heise gauge (Heise, Inc. model 901A-5000), with an accuracy of ±0.34 bar. The *equilibration system* (Figs. 2 and 3) consists of a stainless steel vessel (internal volume of approximate 50 ml), in which an excess of the solid solute is placed. The outlet from the equilibration vessel is connected to the Valco, Inc. sampling valve. Glass wool is placed at the exit of the vessel to prevent particle entrainment. The temperature in the vessel is controlled to ±0.1 K with an Omega Inc. Micromega CN77000 temperature controller. Cartridge heaters are fitted into holes in the vessel wall. In addition, the equilibration vessel and connecting lines are placed inside a constant temperature oven. The total volume of the recirculation system is approximately 32 ml (~25 ml of the equilibration vessel is occupied by glass beads). The *heating system* consists of the cartridge heaters in the equilibration vessel and a constant temperature oven. The cartridge heaters provide initial heating and the oven maintains constant temperature for the whole system. To monitor the temperature, three thermocouples and indicators were placed in the system: a type-T thermocouple for the oven, a type-T thermocouple in contact with the SCF in the equilibration vessel and an RTD thermocouple in the equilibration vessel block. The heating system is crucial for maintaining isothermal operation and avoiding precipitation in the lines. The *sampling system* consists of three valves and exchangeable sample loops (251.6, 503, 1007 and 2002 μl). The Valco, Inc. sampling switching valve model C6WE (placed inside the oven) is connected to the recirculation and venting system (elution position) and to the sampling and cleaning system (load position). The analyte valve is used to deposit the sample into the collection flask and the solvent wash valve is used to inject collection solvent and sweep any possible particles that could have been entrained during the

expansion. The *cleaning/venting system* consists of a taper seal HIP, Inc. vacuum valve (placed in between the Valco valve and the solvent wash valve), that is connected to the CO_2 tank and the vacuum pump for cleaning purposes. For safety and cleaning reasons, there is also a vent valve.

2.3 Apparatus Operation

The equilibration vessel is filled with a large excess of the compound of interest (caffeine, uracil or erythromycin) and glass beads are added to improve mass transfer as the SCF passes through the vessel. The system (including the sample loop) is filled with CO_2 to the desired pressure from the ISCO pump and the CO_2 is pumped through the system with the recirculation pump (10% of the maximum rpm, which provides a pumping rate on the order of 10 ml/min for water). During equilibration the Valco valve is in the *Elute* position, which allows by-passing of the sample loop. After the pressure stabilizes ($\pm$0.14 bar), the temperature controllers and heaters are activated, taking care to avoid temperature overshoot. Once the temperature indicators and pressure gauge confirm an isothermal isobaric system and the system reaches thermodynamic equilibrium (usually 30 - 90 minutes are allowed), the Valco valve is switched to the *Load* position to fill the sample loop with the saturated SC CO_2/solute solution. The recirculation pump is turned off momentarily when the Valco valve is switched between *Elute* and *Load* positions in order to avoid any unnecessary pressure spikes. The Valco valve is switched back to the *Elute* position and the analyte valve opened slowly to expand the sample into a liquid collection solvent (water or ethanol, depending on the solute studied). Once no more bubbles are observed in the collection solvent, the solvent

wash valve is opened and the sample loop is flushed with 4 ml of wash solvent, which is also deposited in the collection vial. The sample is analyzed using a Varian model Cary-1 UV-visible system spectrometer. Before taking the next sample at the same conditions the system is cleaned meticulously by vacuuming the liquid out of the sample collection system and flushing with pure CO_2. At least four replicates are taken at each pressure. When a new solute is used, the entire system is washed thoroughly with a liquid solvent (generally ethanol) and flushed with CO_2 until no residual contamination is detected.

3. Modeling

The solubility model used to represent the high-pressure phase behavior of the three molecules is shown in Eq. 1. This equation is a result of the equifugacity condition between the solid and the fluid phase, under the assumption that the solubility of the solvent (CO_2) is negligible in the solid phase.

$$y_2 = \frac{P_2^{\text{sub}} \phi_2^{\text{sub}}}{P \hat{\phi}_2} \exp\left[\frac{v_2^{\text{M}} \left(P - P_2^{\text{sub}}\right)}{RT}\right] \tag{1}$$

Eq. 1, as explained elsewhere [37, 38], represents the solubility of component 2 (solute) in the supercritical phase. P_2^{sub} is the saturation (sublimation) pressure of component 2 at temperature *T*, ϕ_2^{sub} is the fugacity coefficient at the saturation pressure, $\hat{\phi}_2$ is the fugacity coefficient for the solute in the SCF phase, and v_2^{M} is the molar volume of the solid. In this work $\hat{\phi}_2$ is calculated using the Peng-Robinson equation of state (EOS) with van der Waals mixing rules.

The equifugacity condition represented in this equation is a necessary condition; however, it is not sufficient to guarantee a stable solid-fluid equilibrium result. As discussed by Xu et al. [19], solutions of the equifugacity equation must be tested for global phase stability, given that multiple solutions could satisfy the equifugacity condition but only those that satisfy the stability condition represent the true phase equilibrium. In this work, the methodology discussed by Xu et al. [19] was used to test the stability of the system. This methodology consists of the application of the tangent plane distance criteria [39] and a global minimization technique based on interval analysis [19, 40] that can guarantee the identification of the correct thermodynamically stable composition of a fluid phase in equilibrium with a pure solute.

3.1 Estimation of properties

To calculate the solubility and phase stability of a solute in a supercritical fluid using an EOS it is necessary to have critical properties and acentric factors of all components, and molar volumes and sublimation pressures of the solid components. When some of these values are not available, as is the case here, estimation techniques must be employed. When neither critical properties nor acentric factors are available in the literature, it is desirable to have the normal boiling point (T_b) of the compound since some estimation techniques require only T_b and molecular structure. Also, vaporization, sublimation and/or fusion curves and normal melting point information might be of help for the estimation of T_b. Molar volumes may be available from crystallography studies. Some of the estimation techniques used below, where only the molecular structure and/or

molecular weight are required, are available in ASPEN Properties™ and we have used this tool to estimate the T_b, T_c and P_c of erythromycin.

In the following subsections, different property estimation techniques used in this work will be discussed. We used the estimated T_c, P_c and ω as parameters in the Peng-Robinson EOS; beyond that we do not assign any physical significance to the values obtained. The properties found in the literature or estimated with the methods explained below are summarized in Table 1. Note that with the objective of obtaining the best fit of the solubility behavior of the three solutes in supercritical CO_2, there are at least two different sets of properties reported for each component, depending on the estimation method used. They are described more specifically in the corresponding results and discussion sections.

3.1.1 Boiling Point

As mentioned above, the normal boiling point of a component is one of the key properties for the estimation of other parameters or properties. Two methods were used to estimate boiling points: the Joback group contribution approach, as presented in Reid et al. [41] and the Meissner approximation [42], a correlation that depends on molar refraction $[R_D]$, parachor $[P]$ and *B*, a constant whose value depends upon the chemical type. Values of these parameters are explained in more detail in Lyman et al. [43]. The Meissner method was particularly useful for estimating the boiling point of erythromycin, given that the Joback group contribution approach (ASPEN Properties™ value) produced an obvious overestimation of T_b. This is not surprising, since the Joback method was not originally

designed for such large molecules. For caffeine, T_b was already available in the literature so no estimation technique was needed. For uracil, T_b was estimated using the Joback contribution approach, along with the sublimation curve and melting point data.

3.1.2 Critical Properties and Acentric Factors

Critical properties are crucial for an accurate representation of experimental behavior. In this work, three methods were used to estimate these properties: the Fedors and Joback group contribution approaches described in detail by Reid et al. [41] and the Ambrose method described by Reid et al. [41] and Perry et al. [44].

For caffeine, the Fedors and Joback group contribution approaches were utilized, as had been done previously [37, 38]. For uracil, these same two methods were applied, but for erythromycin all three methods were used, with the objective of finding the best fit for the experimental data. Where possible, the values presented were estimated with ASPEN Properties™ ver. 11.1. Since erythromycin is not included in the ASPEN database, it was necessary to input the molecular structure drawn in ISIS Draw ver. 2.4 and introduce the molecular weight and/or the Meissner estimated value of the boiling point. More details are discussed in section 4.3.

Acentric factors, ω, for all molecules were estimated using a correlation based on Antoine's vapor pressure equation. In addition, for erythromycin, the Lee-Kesler correlation was used. As it will be discussed in section 4.3, no major improvements for

erythromycin were found with the latter correlation. Both correlations are described in Reid et al. [41].

3.1.3 Sublimation pressure

The sublimation pressure for caffeine and uracil were available in the literature. However no data has been reported for erythromycin. Therefore the Watson correlation for solids [45], as described in Lyman et al. [43], was used. The value of K_F, the Fishtine constant used in this correlation, for erythromycin was 1.06 (the default value) and $\Delta Z_b = 0.97$, as assigned previously [43].

3.1.4 Molar volumes

Molar volumes of the three molecules were found in the literature and their values and references are reported in Table 1. For erythromycin, the value was approximated by the difference between the molar volume of erythromycin A ($C_{37}H_{71}NO_{15}$) [46], a hydrated form, and the molar volume of water in the solid state, in order to provide a rough estimate of the real density of erythromycin ($C_{37}H_{67}NO_{13}$).

3.1.5 k_{ij} interaction parameters

The interaction parameters between the three molecules and carbon dioxide at each temperature were obtained by regression of the experimental data and the values are shown in Table 2. The objective function used was the average absolute relative deviation (%AARD), as shown in Eq. 2. Here y_i^{exp} are the experimental data, y_i^{calc} are the predicted values and *n* is the total number of data points.

$$\%\text{AARD} = \frac{100}{n}\sum_{i=1}^{n}\frac{\left|y_{\text{i}}^{\text{exp}} - y_{\text{i}}^{\text{calc}}\right|}{y_{\text{i}}^{\text{exp}}} \quad (2)$$

4. Results and discussion

In this section, experimental measurements and modeling results of the solubility of caffeine, uracil and erythromycin in SC CO_2 are presented. Also included is a discussion of the various property estimation techniques.

4.1 Solubility of caffeine in SC CO_2

Solubility measurements of caffeine were performed at 40 °C for a pressure range of 100 to 300 bar. Previously, several authors [15-17, 20, 21, 47-49] have presented results for caffeine solubility in SC CO_2 at various conditions (Table 3). In Table 4 and Fig. 4 the results from this study are compared with the literature values at 40 °C. Some of the published values [20] were available only in graphical form so those points in Fig. 4 are approximate. The values obtained in this work fall in the range of the values reported by other researchers. Johannsen and Brunner [16], whose values are a bit higher than those obtained here, suggested the somewhat lower values presented by Li et al. [15] might be due to insufficient time being allowed for equilibration during dynamic measurements. For this reason, we performed an initial study to determine the required equilibration (recirculation) time for our system and found that 50 minutes were sufficient. Therefore, in our experiments, samples were collected every 70 minutes to ensure that equilibrium saturation was achieved. With these measurements we were able to validate the experimental technique used for solubility determination. From replicate measurements, we estimate our experimental uncertainty to be ~10%.

The experimental results found were modeled using Eq. 1 and the two different sets of parameters shown in Table 1 (set 1 and set 2) and the binary interaction parameters shown in Table 2. Note that critical properties and the acentric factor of set 1 were estimated by other authors [15, 50] using the Joback method. The k_{ij} parameter (-0.0602) was estimated from a combination of the experimental data from this study and that of Li et al. [15]. Set 2 consists of parameters estimated with the Fedors and Ambrose methods and these were presented by Mehr et al. [14]. Once again the k_{ij} parameter (-0.4348) was estimated from a combination of the experimental data from this study and that of Li et al. [15]. The sublimation pressure for both sets was calculated using Eq. 3, which is taken from Bothe et al. [50].

$$\log_{10} P^{\text{sub}} = 15.031 - \frac{5781}{T}, \quad T\,[=]\,\text{K},\ P\,[=]\,\text{Pa} \tag{3}$$

The modeled solubilities using set 1 have a %AARD of 36.9 and for set 2, a %AARD of 16.3 was obtained. As seen in Fig. 5 the Peng-Robinson equation represents the experimental behavior of the system quite well, especially using the properties corresponding to set 2, although this set requires a much larger negative k_{ij} value. The largest deviations between experimental and modeled values are found at lower pressures for both sets of parameters. All modeling results presented here were tested for phase stability using the interval methodology proposed by Xu et al. [19].

4.2 Solubility of uracil in SC CO_2

Uracil solubility measurements were performed at 40 °C and 60 °C for pressures between 100 and 300 bar. As shown on Table 5, the experimental solubilities are from 10^{-6} to 10^{-4} mole fraction. The solubility at the lowest pressures are quite low but the solubility increases rapidly with increasing pressure. The solubility at 60 °C is higher, no doubt due to the higher solid saturation pressure at this temperature. The use of protic cosolvents, with the possibility of hydrogen bonding with the ketone groups, might be able to increase the solubility of uracil even further but this was not included in this study. The estimated uncertainty from replicate measurements is ~15%.

The experimental results were modeled using the Peng-Robinson EOS using two different sets of parameters. The sublimation pressure for both sets was estimated using the following correlation (Eq. 4) found in Brunetti et al. [51].

$$\log_{10} P^{\text{sub}} = 12.29 - \frac{6634}{T}, \quad T\,[=]\text{K},\ P\,[=]\text{kPa} \tag{4}$$

For both sets, critical constants and the acentric factor were calculated using the Joback contribution method approach. However, given that the boiling point (T_b) is required for these estimations and was not available in literature, T_b was estimated using two different approaches. For the first set, set 1, T_b was estimated recalling the thermodynamic relation expressed in Eq. 5. It is assumed that $\Delta Z_V = 1$ (the molar volume of the liquid is negligible compared to the molar volume of the vapor) and that the normal melting point (T_f = 338 °C [24]) is a reasonable estimate of the triple point temperature (T_{TP}). The typical pure component phase diagram shown in Fig. 6 makes clear why this assumption

is made. Then the sublimation pressure equation (Eq. 4) was used to obtain the pressure at T_{TP}. The value obtained was used as a reference point from which to extend the vaporization curve (Eq. 5 and 6), knowing ΔH_v=83.736 kJ/mol [52]. The rough estimation of the boiling point by this method is 391 °C.

$$\frac{d \ln P^{vap}}{d\left(1/T\right)} = -\frac{\Delta H_v}{R \Delta Z_v} \tag{5}$$

$$\ln P^{vap} = 26.69 - \frac{10071.69}{T}, \quad T[=]\text{K}, \; P[=]\text{Pa} \tag{6}$$

T_b for set 2 was estimated following the Joback contribution approach. The value found, 274 °C, differs significantly from the first approach and is not physically reasonable since it gives a normal boiling point that is less than the experimentally known normal melting point. However, set 2 is included here to emphasize the dramatic differences that one can obtain using different estimation techniques.

The binary interaction parameters at 40 °C and at 60 °C were estimated from the experimental data obtained in this study. Figs. 7 and 8 present a comparison of the experimental and modeling results at 40 °C and 60 °C, respectively, using both sets of parameters. As seen from the figures, the Peng-Robinson equation represents the experimental behavior of the system quite well with both sets of parameters at pressures greater than 200 bar; however, at lower pressures the error is greater than 60%. Due to these discrepancies at lower pressures, the %AARD at 40 °C is ~37% for set 1 and ~44% for set 2. The %AARD at 60 °C is ~46% for set 1 and ~48% for set 2. Set 1 parameters are no doubt the better set given that the boiling point was estimated using enthalpy of

vaporization data. Moreover, the binary interaction parameters are more reasonable for set 1 and the %AARD is slightly better. As in the previous case, both sets of results were tested for stability to make sure that the modeling results presented are correct.

4.3 Solubility of erythromycin in SC CO_2

Erythromycin solubility measurements were performed at 40 °C and 60 °C and at pressures from 150 to 300 bar. Since erythromycin is highly hygroscopic and its extinction coefficient in the UV-Vis region is quite small, some adjustments in the operating procedure were made. First, erythromycin was dried for ~12 hours in a vacuum oven and placed and sealed in the extraction vessel in a glove box. Also, special care was taken to ensure that there were no leaks in the system that could allow contact of the erythromycin with humid air. Second, due to the small extinction coefficient and low solubilities at pressures lower than 200 bar, larger sample loops (1007 µl and 2002 µl) and smaller amount of collection solvent (ethanol) were used. However, absorbances for experiments at pressures below 150 bar were still below the detection limit, which we estimate to be 1.1×10^{-4} and 1.7×10^{-4} mole fraction at 40 and 60 °C respectively. The experimental results, shown in Figs. 9 and 10 and Table 6, show solubilities in SC CO_2 in the range of 10^{-4} to 10^{-3} mole fraction at pressures from 150-300 bar. The solubilities found at high pressures are remarkably high considering the large size of the molecule. Perhaps this is related to the unusual interaction of erythromycin with CO_2, as has been noted by other researchers [29-31]. The results are completely reproducible, with an estimated uncertainty from replicate measurements of ~16%.

Modeling of erythromycin was particularly difficult. Although this is a molecule that has been widely studied from a biological and clinical point of view, little information has been disclosed in terms of thermodynamic properties. Given that neither sublimation pressure nor critical constants are available, several group contribution estimation methods were used. The Meissner approximation and the Joback method were used to estimate erythromycin's T_b. The Fedors, Joback and Ambrose methods, described previously, were used to estimate the critical properties using ASPEN Properties™ ver. 11.1. Given that erythromycin is not part of the ASPEN database, the molecule was drawn first in ISIS™/Draw 2.4© and then imported into ASPEN where, in addition, the molecular weight and/or the Meissner boiling point were specified. A summary of these parameters, their origin, estimated k_{ij} values and the %AARD values produced with each set are listed in Tables 7 and 8. Interaction parameter values were estimated from regression of the experimental data and the sublimation pressure was estimated using the Watson correlation for solids with the parameters mentioned in section 3.1.3. The values for the sublimation pressure are quite small; this is likely due to an overestimation of the boiling point, which is used as a parameter in the Watson correlation. In Table 7 it can be observed that the acentric factors estimated in sets 3-5 are positive and, thus, might have some physical significance (measure of nonsphericity of the molecule). Given that erythromycin is a high-molecular-weight molecule, one would expect ω to have a large positive value. The Lee-Kesler method was also used for the estimation of ω, but only small improvements in the model were found; therefore, we are not including those results here.

Set 1 corresponds to results using T_b estimated with the Joback method. The apparent overprediction of T_b produces a correspondingly large T_c, which is much higher than the values estimated with other methods. From Table 8 one can see that only sets 3-5 give reasonable values of k_{ij}. Graphical results of all models at 40 and 60 °C are shown in Fig. 9 and 10. From Fig. 9, it is clear that sets 1, 2 and 3 do not even represent the correct qualitative behavior of the solubility of erythromycin in SC CO_2 at 40 °C. By comparison, sets 4 and 5 provide more reasonable estimates of the solubility up to 250 bar but predict a slight decrease in solubility at the highest pressures, which is not observed experimentally. Set 4 corresponds to properties estimated with the Meissner and Ambrose methods and set 5 corresponds to properties estimated with the Meissner, Fedors and Ambrose methods (Table 7). Both sets of properties fit the experimental behavior at 40 °C equally well (%AARD values of 15.6 and 8.1, respectively). In Fig. 10, results at 60 °C are presented. As seen in table 8, all five sets of parameters yield reasonable %AARD values. However, none of the sets of parameters yield satisfactory results. Although they seem to capture the correct qualitative behavior, sets 1 and 2 require ridiculous k_{ij} values. Sets 3-5 show increasing solubility with increasing pressure but seriously underpredict the solubility at the lower pressures. These results emphasize the importance of the parameter estimation techniques, especially for large solute molecules. Relatively small variations in the estimated parameters can cause large differences in the predicted solubilities. For instance, sets 3 and 4 differ by just 20 °C in T_c and 1.4 bar in P_c but yield large differences in the solubility predictions. It is important to note that the poorer quality modeling observed for erythromycin is not surprising since it is the largest solute studied and all parameters, as well as the sublimation pressure, had

to be estimated. The sublimation pressure is very small and, therefore, one can legitimately question the accuracy of the Watson Correlation in this pressure range [43]. For systems like this, experimental data is certainly of the utmost importance. Moreover, it is clear that the Peng-Robinson EOS is not the best choice for this system. As before, the modeling results were tested for stability to ensure that they satisfied both the equifugacity and phase stability criteria.

5. Conclusions

In this study, we presented measurements and modeling of the solubility of caffeine, uracil and erythromycin in supercritical CO_2 at 40 and 60 °C and pressures up to 300 bar. Caffeine solubility was used to validate the experimental apparatus and technique. The solubility of uracil, a nucleic acid base, in SC CO_2 increased with increasing pressure and increasing temperature, falling in the range of 2.9×10^{-6} to 1.3×10^{-4} mole fraction. The solubility of erythromycin, an antibiotic, is relatively high (up to 2.1×10^{-3} mole fraction) compared to that of uracil, especially considering its large size. The Peng-Robinson equation with van der Waals mixing rules was used successfully to model the solubilities of caffeine and uracil, accurately representing the phase behavior. Modeling of erythromycin was significantly more difficult due to the lack of physical property information. However, estimation techniques such as the Meissner method and Watson Correlation for T_b and P^{sub}, respectively, were quite helpful in obtaining rough, order of magnitude, estimates of the solubility. It is also important to highlight that small changes in critical properties estimated can cause large changes in the solubility estimates. In all

cases, the modeling results were checked, using interval analysis, to ensure that they satisfied phase stability, as well as the necessary equifugacity requirement.

Acknowledgments

The authors are grateful to The State of Indiana 21st Century Fund Grant for financial support of this project. In addition, we thank Dr. Aaron Scurto for helpful discussions.

List of symbols

%AARD	average absolute relative deviation
B	constant for Meissner approximation according to chemical type
ΔH	enthalpy
k_{ij}	binary interaction parameter of component *i* and *j* for Peng-Robinson EOS
K_{F}	Fishtine constant
P	pressure
$[P]$	Parachor number
R	universal gas constant
$[R_{\mathrm{D}}]$	molar refraction
T	temperature
v^{M}	molar volume of the solid
y_{i}	solubility of the solute
ΔZ	compressibility factor

Greek letters

ϕ	fugacity coefficient
ω	acentric factor

Subscript

2	solute
b	boiling
c	critical
f	fusion, melting
i, j	component indices
TP	triple point
v	vaporization

Superscript

calc	calculated
exp	experimental
sub	sublimation
vap	vapor
™	trademark
©	copyright

References

1. Wong, J.M. and K.P. Johnston, Biotechnol. Prog., **2** (1986) 29-39.

2. Kim, J.R. and H. Lentz, Fluid Phase Equilib., **41** (1988) 295-302.

3. Fornari, R.E., P. Alessi and I. Kikic, Fluid Phase Equilib., **57** (1990) 1-33.

4. Knudsen, K., L. , L. Coniglio and R. Gani, ACS Sym Ser., **608** (1995) 140-153.

5. Dohrn, R. and G. Brunner, Fluid Phase Equilib., **106** (1995) 213-282.

6. Macnaughton, Stuart J., I. Kikic, N.R. Foster, P. Alessi, A. Cortesi and I. Colombo, J. Chem. Eng. Data, **41** (1996) 1083-1086.

7. Cross Jr., W., A. Akgerman and C. Erkey, Ind. Eng. Chem. Res., **35** (1996) 1765-1770.

8. Cassel, E. and J.V. de Oliveira, J. Supercrit. Fluids, **9** (1996) 6-11.

9. Smart, N.G., T. Carleson, T. Kast, A.A. Clifford, M.D. Burford and C.M. Wai, Talanta, **44** (1997) 137-150.

10. Reverchon, E. and G. Della Porta, Powder Technol., **106** (1999) 23-29.

11. Ko, M., V. Shah, P.R. Bienkowski and H.D. Cochran, J. Supercrit. Fluids, **4** (1991) 32-39.

12. Gordillo, M.D., M.A. Blanco, A. Molero and E. Martinez de la Ossa, J. Supercrit. Fluids, **15** (1999) 183-190.

13. Maxwell, R.J., J.W. Hampson and M.L. Cygnarowicz-Provost, J. Supercrit. Fluids, **5** (1992) 31-37.

14. Mehr, C.B., R.N. Biswal and J.L. Collins, J. Supercrit. Fluids, **9** (1996) 185-191.

15. Li, S., G.S. Varadarajan and S. Hartland, Fluid Phase Equilib., **68** (1991) 263-280.

16. Johannsen, M. and G. Brunner, Fluid Phase Equilib., **95** (1994) 215-226.

17. Saldaña, M.D.A., R.S. Mohamed, M.G. Baer and P. Mazzafera, J. Agric. Food Chem., **47** (1999) 3804-3808.

18. Willson, R.C. and C.L. Cooney, Abstr. Pap. Am. Chem. S., **190** (1985) 158-MBD.

19. Xu, G., A.M. Scurto, M. Castier, J.F. Brennecke and M.A. Stadtherr, Ind. Eng. Chem. Res., **39** (2000) 1624-1636.

20. Stahl, E. and W. Shilz, Talanta, **26** (1979) 675-679.

21. Gährs, H.J., Ber Bunsen-Ges Phys Chem Chem, **88** (1984) 894-897.

22. Banks, J.F. and C.M. Whitehouse, Int. Mass Spectrom. Ion Processes, **162** (1997) 163-172.

23. Davies, R.G., V.C. Gibson, M.B. Hursthouse, M.E. Light, E.L. Marshall, M. North, D.A. Robson, I. Thompson, A.J.P. White, D.J. Williams and P.J. Williams, J. Chem. Soc., Perkin Trans. 1, **24** (2001) 3365-3381.

24. Baker, E.A., A.L. Hayes and R.C. Butler, Pestic. Sci., **34** (1992) 167-182.

25. Zielenkiewicz, W., J. Poznanski and A. Zielenkiewicz, J. Solution Chem., **29** (2000) 757-769.

26. Ganguly, S. and K.K. Kundu, Journal of Phys., **41** (1993) 10862-10867.

27. Ganguly, S. and K.K. Kundu, Indian J. Chem., Sect. A, **34** (1995) 857-865.

28. Ganguly, S. and K.K. Kundu, Indian J. Chem., Sect. A, **35** (1996) 423-426.

29. Goldstein, E.J.C., L.S. Vera, Y. Kwok and L.R. P., Antimicrob. Agents and chemother., **20** (1981) 705-708.

30. Hansen, S.L., P. Swomley and G. Drusano, Antimicrob. Agents and chemother., **19** (1981) 335-336.

31. Goldstein, E.J.C. and L.S. Vera, Antimicrob. Agents and chemother., **23** (1983) 325-327.

32. Jayaraman, S.C., C. Ramachandran and N. Weiner, J. Pharm. Sci., **85** (1996) 1082-1084.

33. Yudi, L.M., A.M. Baruzzi and V. Solis, J. Electroanal. Chem., **360** (1993) 211-219.

34. Scurto, A.M., High-Pressure Phase and chemical equilibria of β-Diketone ligands and chelates with carbon dioxide, Ph D Thesis, University of Notre Dame, Notre Dame, 2002.

35. Wendland, M., H. Hasse and G. Maurer, J. Supercrit. Fluids, **6** (1993) 211-222.

36. Adrian, T., H. Hasse and G. Maurer, J. Supercrit. Fluids, **9** (1996) 19-25.

37. Smith, J.M., H.C. Van Ness and M.M. Abbott, *Introduction to Chemical Engineering Thermodynamics*. 5th ed. Chemical Engineering Series. Mc Graw Hill: New York, 1996.

38. Prausnitz, J.M., N.L. Rüdiger and E. Gomes de Azevedo, *Molecular thermodynamics of fluid-phase equilibria*. Third edition ed. Prentice Hall International Series, 1999.

39. Baker, L.E., A.C. Pierce and K.D. Lukus, Soc. Petrol, Eng. J, **22** (1982) 732-742.

40. Hua, J.Z., J.F. Brennecke and M.A. Stadtherr, Fluid Phase Equilib., **116** (1996) 52-59.

41. Reid, R.C., J.M. Prausnitz and B.E. Poling, *The Properties of Gases and Liquids*. 4th ed. McGraw-Hill: New York, 1987.

42. Meissner, H.P., Chem. Eng. Prog., **45** (1949) 149-153.

43. Lyman, W.J., W.F. Reehl and R.D. H., *Handbook of Chemical Property Estimation Methods. Environmental Behavior of Organic Compounds*. Mc Graw-Hill Book Company: New York, 1982.

44. Perry, R.H. and D.W. Green, *Perry's Chemical Engineer's Handbook*. 7th ed. McGraw-Hill companies, Inc.: New York, 1999.

45. Watson, K.M., Ind. Eng. Chem., **35** (1943) 398.

46. Stephenson, G.A., J.G. Stowell, P.H. Toma, R.R. Pfeiffer and S.R. Byrn, J. Pharm. Sci., **86** (1997) 1239-1244.

47. McHugh, M.A. and V.J. Krukonis, *Supercritical Fluid Extraction: Principles and Practice*, ed. Butterworth: Boston, 1986.

48. Lentz, H., M. Gehrig and J. Schulmeyer, Physica B & C ***check, **139** (1986) 70-72.

49. Ebeling, H. and E.U. Franck, Ber Bunsen-Ges Phys Chem Chem, **88** (1984) 862-865.

50. Bothe, H. and H.K. Camenga, J. Term. Anal., **16** (1979) 267-275.

51. Brunetti, B., V. Piacente and G. Portalone, J. Chem. Eng. Data, **45** (2000) 242-246.

52. Clark, L.B., G.G. Peschel and I. Tinoco Jr., J. Phys. Chem., **69** (1965) 3615-3618.

53. Grasselli, J.G. and W.M. Ritchey, *Atlas of Spectral Data and Physical Constants for Organic Compounds*. 2nd. ed. Vol. III. CRC: Cleveland, OH, 1975.

54. Kilday, M.V., J. Res. Natl. Bur. Stand. (U.S.), **83** (1978) 547-554.

55. Teplitsky, A.B., I.K. Yanson, O.T. Glukhova, A. Zielenkiewicz, W. Zielenkiewicz and K.L. Wierchowski, Biophys. Chem., **11** (1980) 17-21.

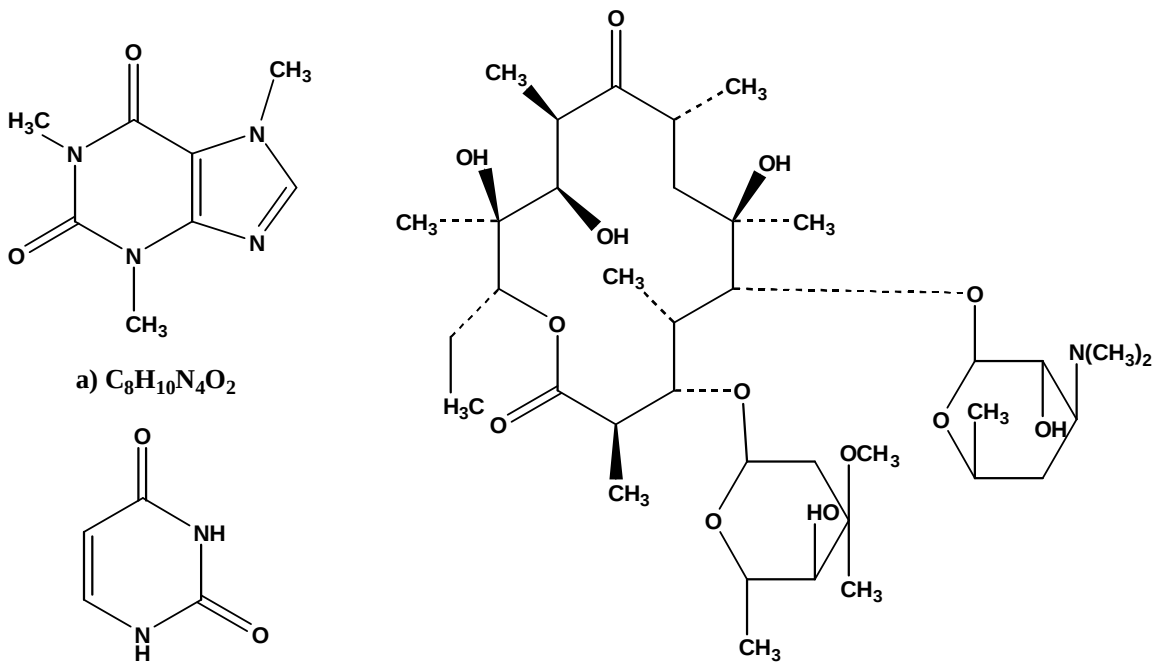

Fig. 1 Solutes studied: a) caffeine, b) uracil, c) erythromycin.

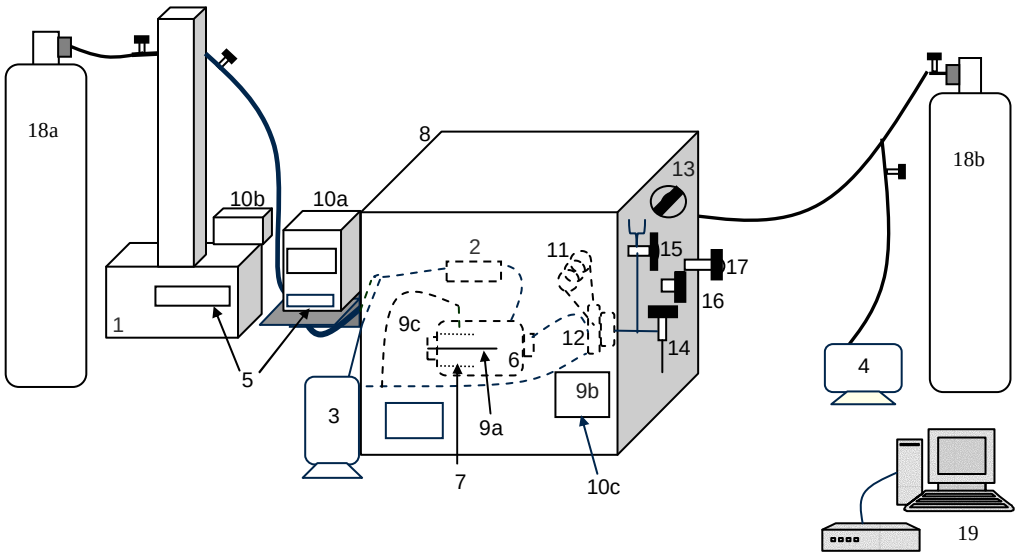

Fig. 2 Detailed schematic of SFE system. *Pumping System:* 1. ISCO syringe pump, 2. check valve, 3. recirculation pump, 4. vacuum pump, 5. pressure indicators. *Equilibration System:* 6. equilibration vessel (see Fig. 3 for details). *Heating System:* 7. cartridge heaters, 8. constant temperature oven, 9. thermocouples (a. type T, oven; b. type T, center of extraction vessel; c. type RTD, cartridge hole) , 10. temperature indicators (a, b and c). *Sampling System:* 11. sample loop, 12. Valco. Inc. sampling switching valve, 13. Valco valve positioner (elution or load), 14. analyte valve, 15. solvent wash valve. *Cleaning/venting system:* 16. vacuum valve, 17. venting valve. *Others:* 18. CO_2 tanks (a & b). 19. Uv-vis-system spectrometer.

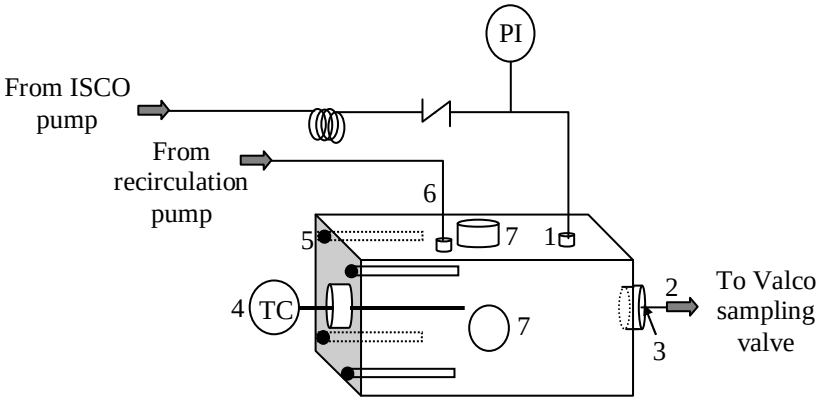

Fig. 3 Detail of equilibration vessel: 1. inlet , 2. outlet, 3. glass wool, 4. temperature controller, 5. cartridge holes, 6. recirculation inlet, 7. glass windows.

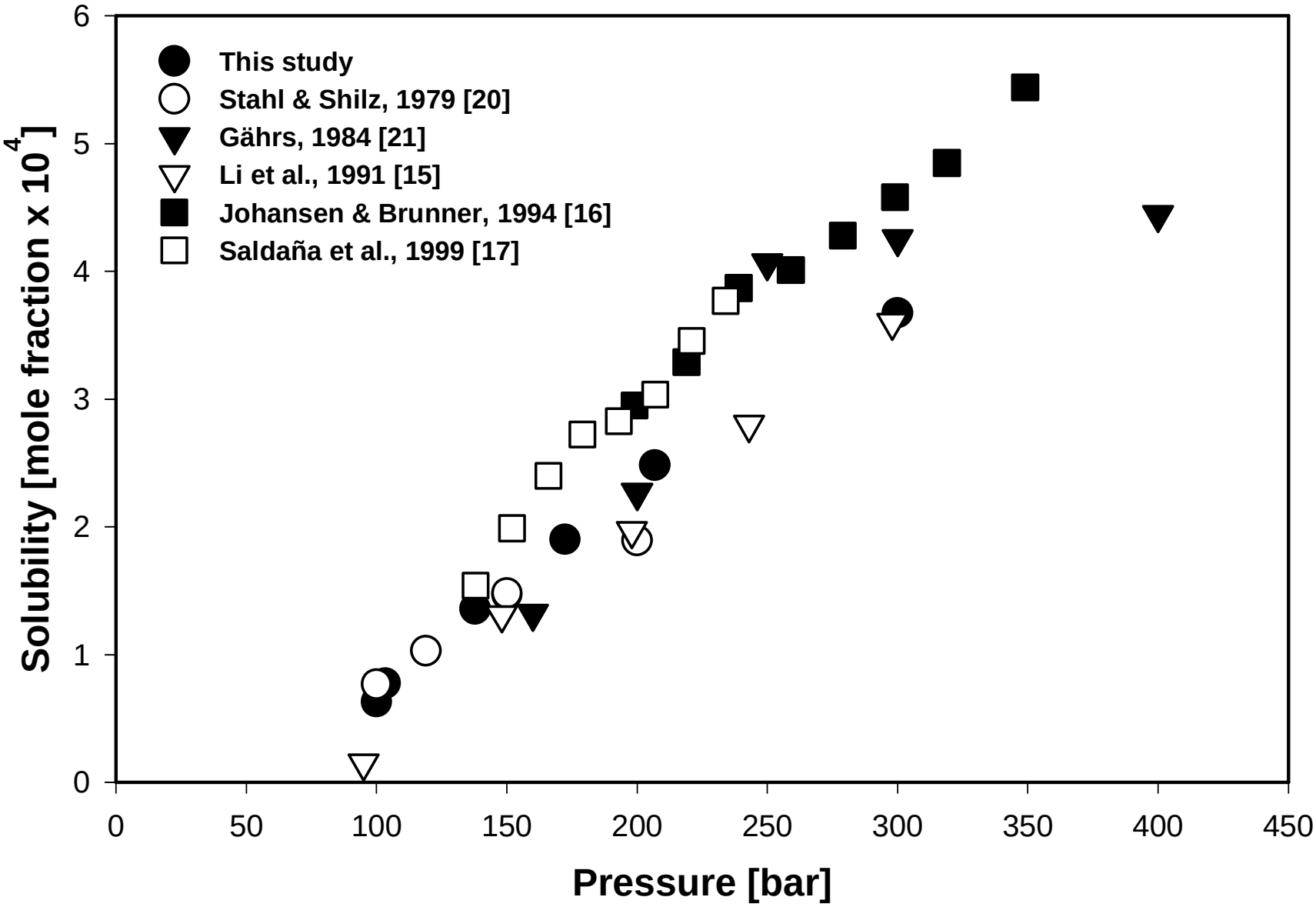

Fig. 4 Experimental and modeled solubilities of caffeine in SC CO_2 at 40 °C.

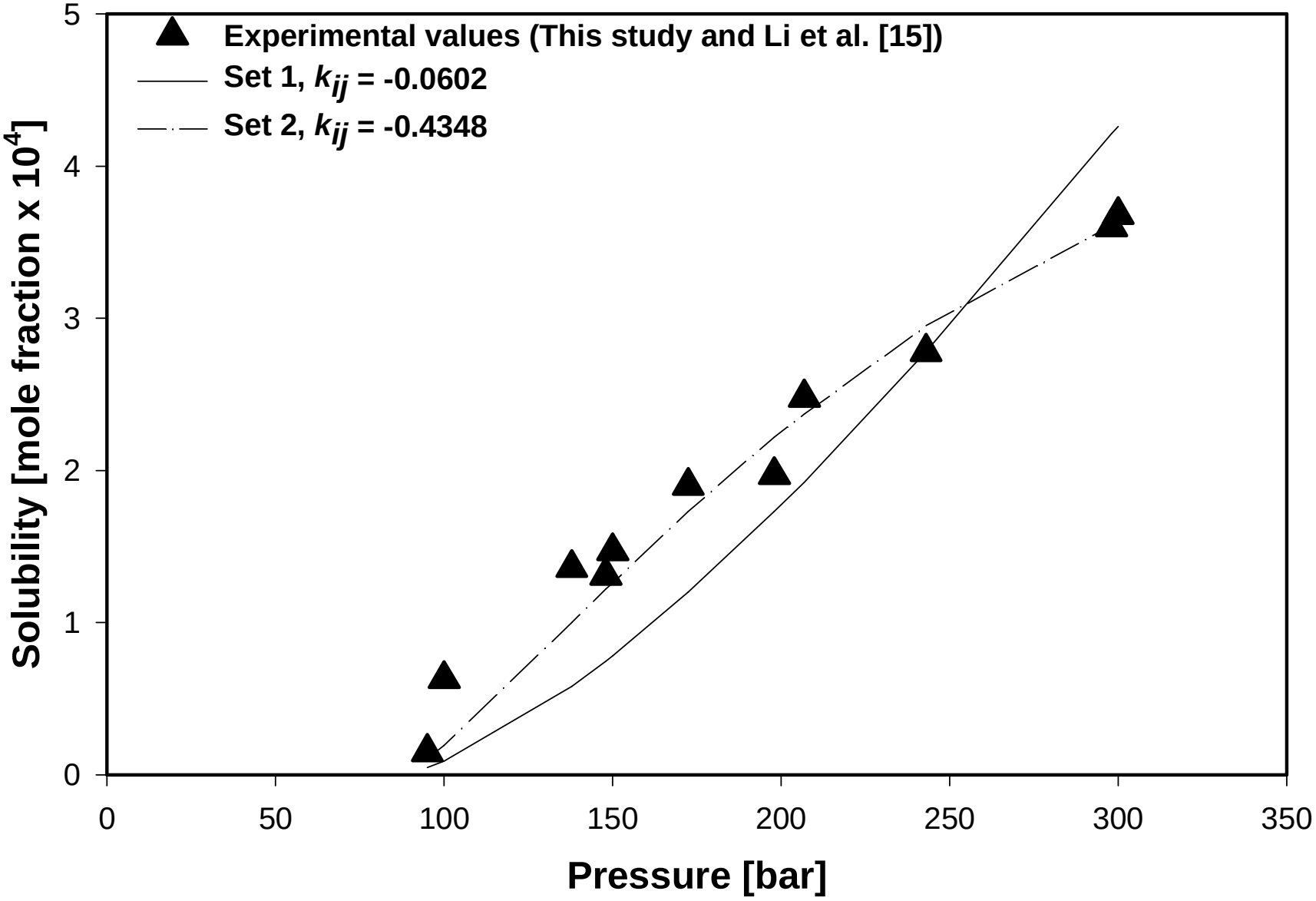

Fig. 5 Solubility of caffeine in SC CO_2 at 40 °C.

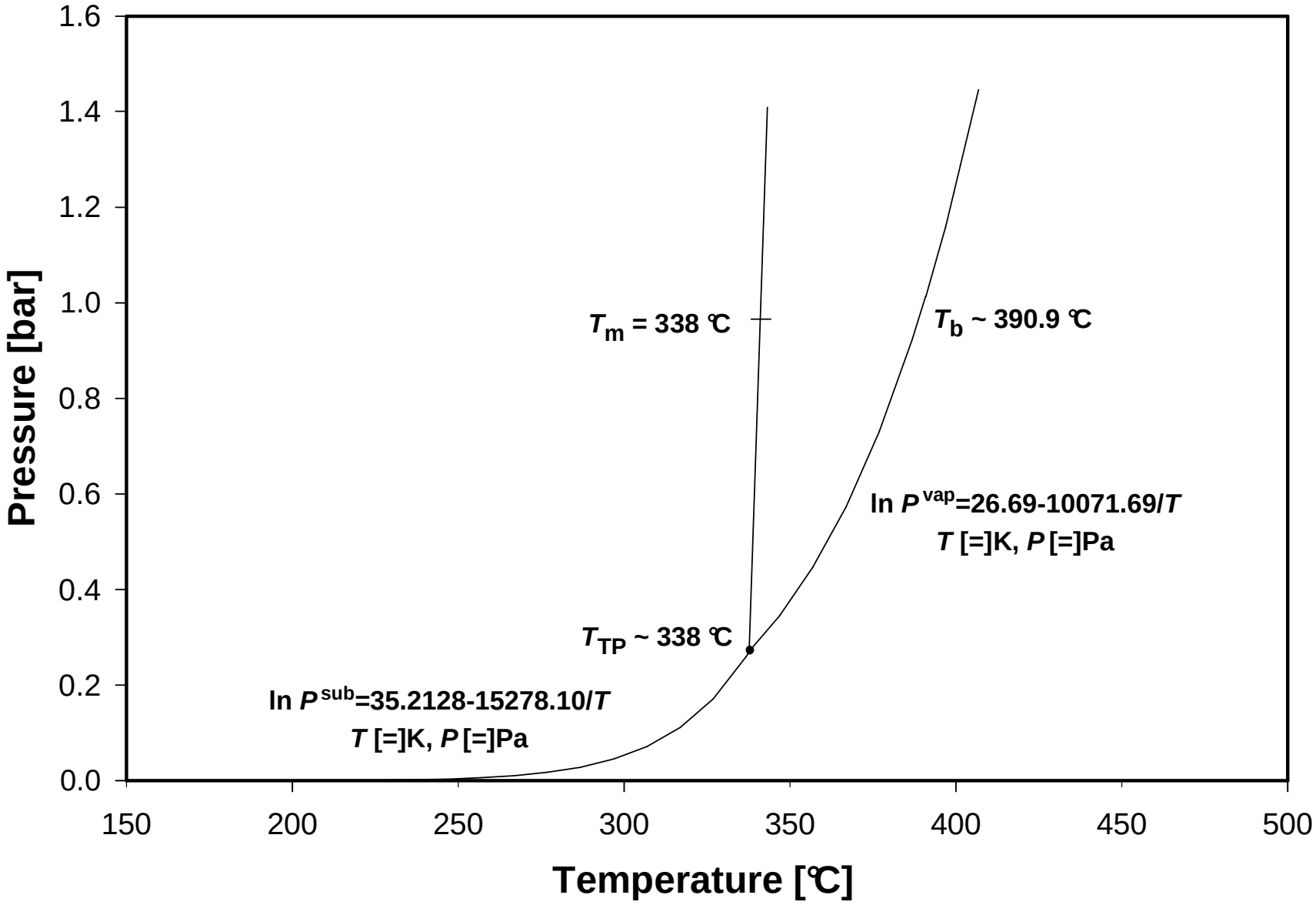

Fig. 6 Schematic of how the boiling point of uracil was estimated (1 Pa = 1 x 10^{-5} bar).

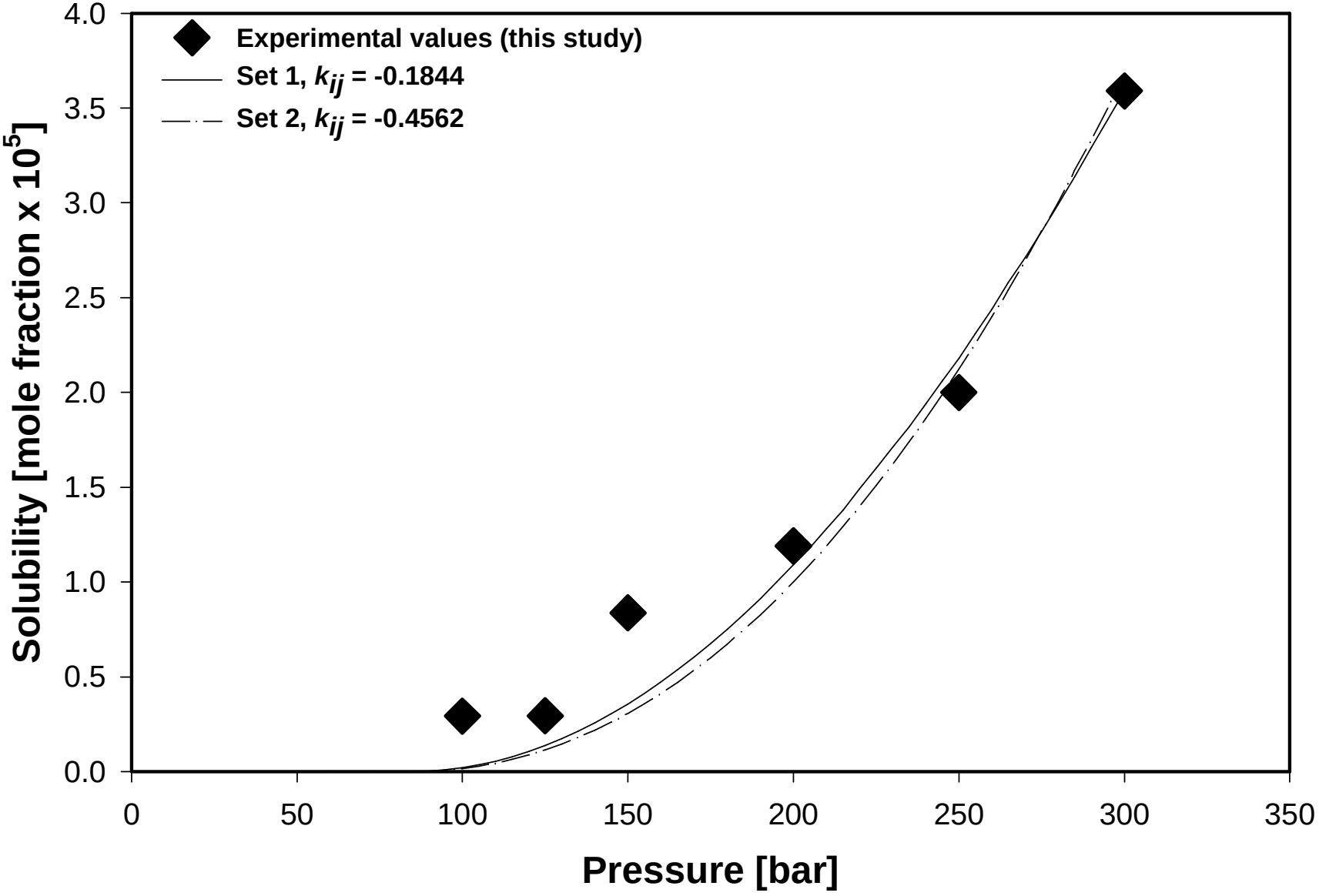

Fig. 7 Comparison of experimental and modeled solubilities of uracil in SC CO_2 at 40 °C using two different sets of parameters.

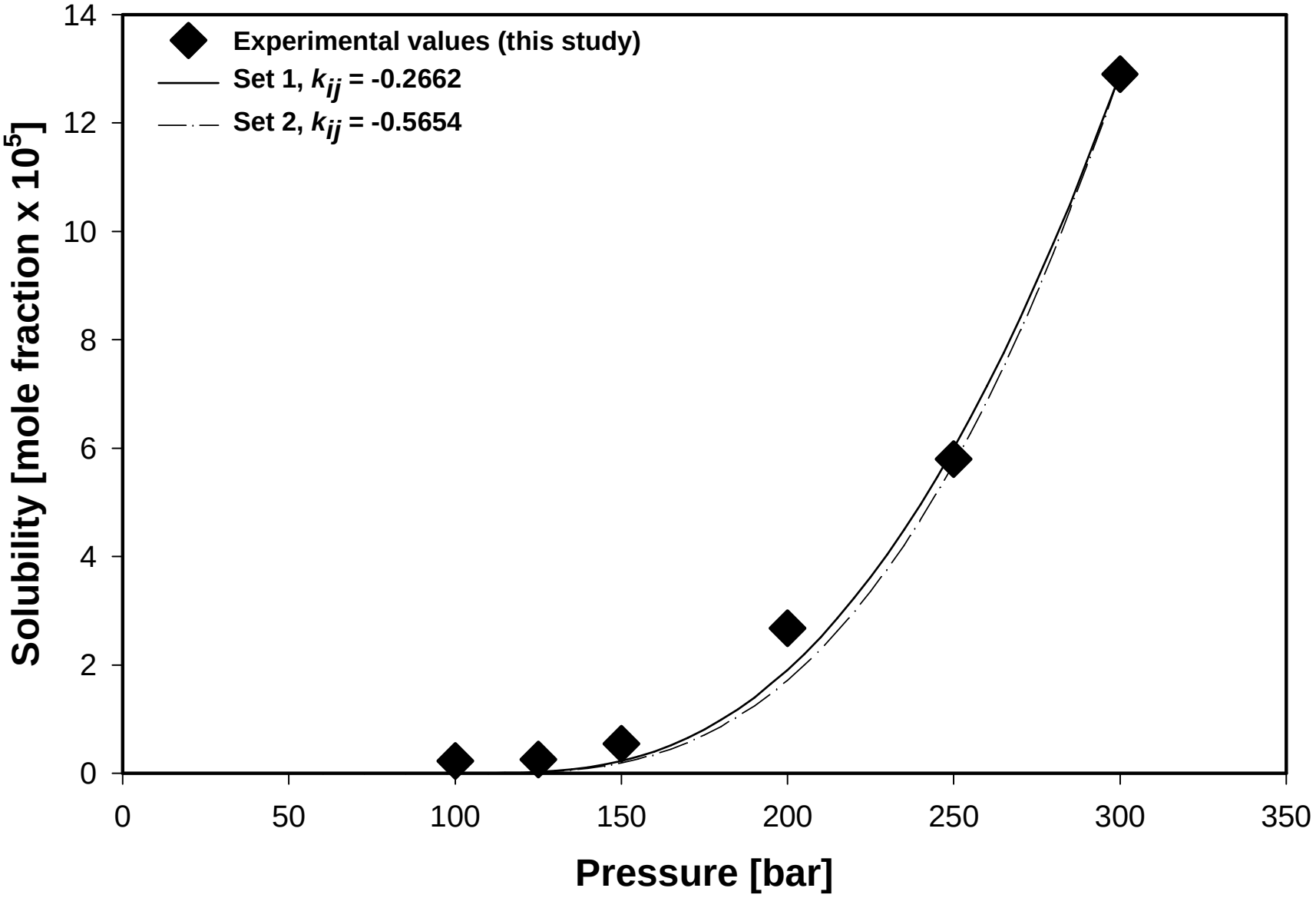

Fig. 8 Comparison of experimental and modeled solubilities of uracil in SC CO_2 at 60 °C using two different sets of parameters.

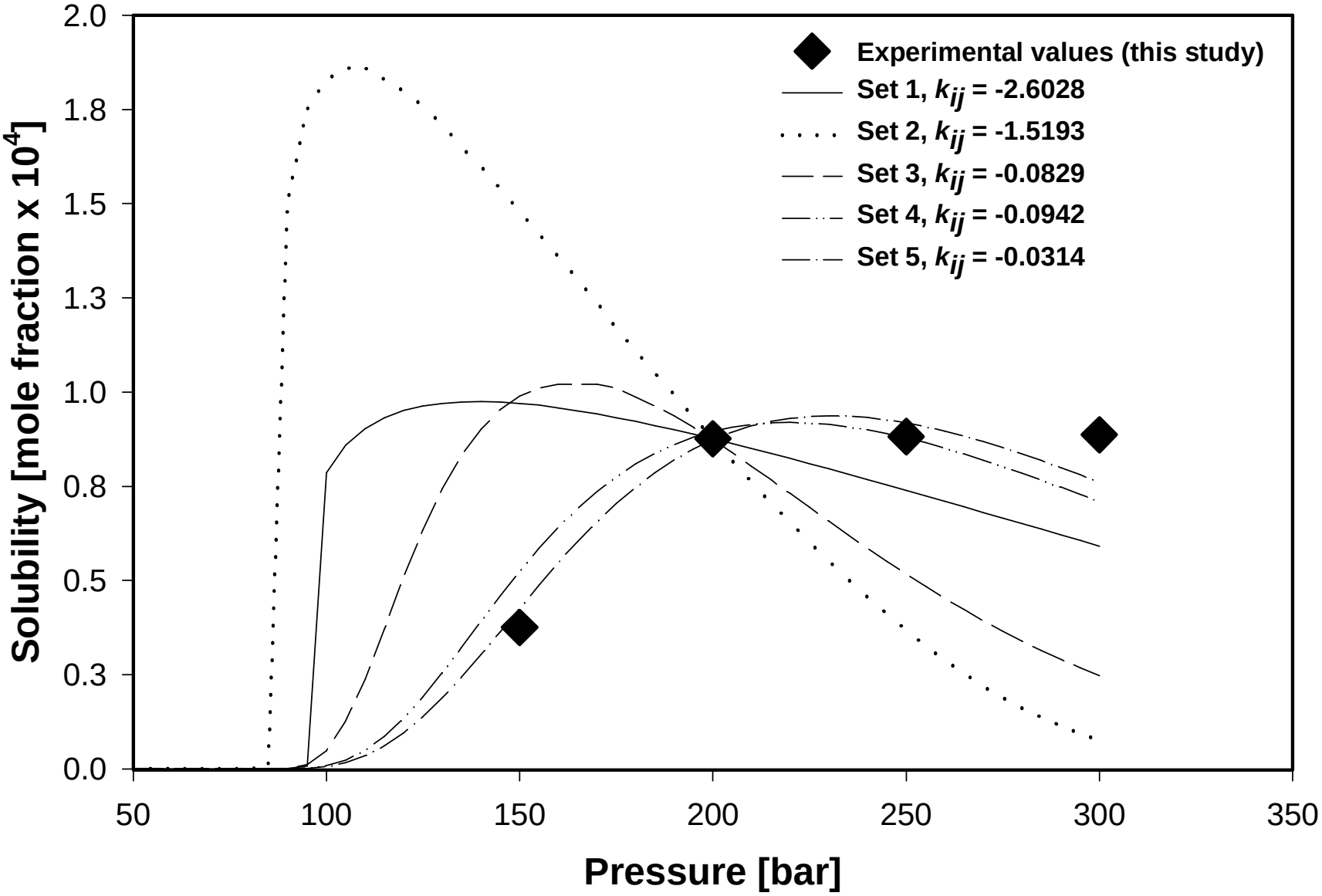

Fig. 9 Comparison of experimental and modeled solubilities of erythromycin in SC CO_2 at 40 °C using several different sets of parameters.

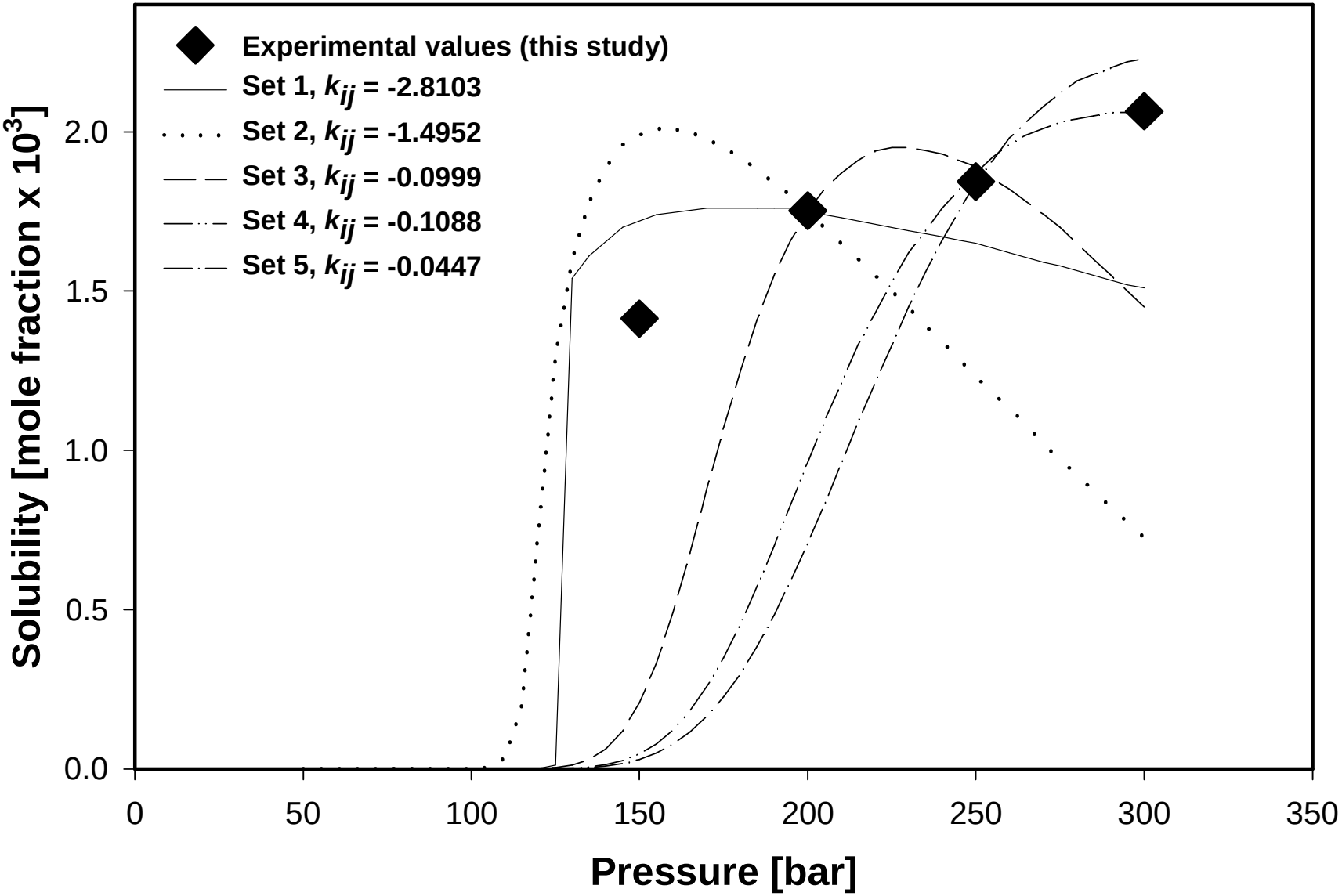

Fig. 10 Comparison of experimental and modeled solubilities of erythromycin in SC CO_2 at 60 °C using several different sets of parameters.

Table 1 Physical properties of the compounds studied

Compound	T_b [K]	T_c [K]	P_c [bar]	ω	P^{sub} [bar] 40 ºC	P^{sub} [bar] 60 ºC	v^M [cc/mol]
CO_2		304.2	73.8	0.225			
Caffeine							
Set 1 [15, 19, 50]		855.6	41.5	0.555	3.7E-09	-	145.7
Set 2 [14, 53]		608.7	20.3	0.247	3.7E-09	-	157.9
Uracil							
Set 1 [51, 54, 55]	664.0	991.3	68.5	0.596	1.3E-11	2.4E-10	68.8
Set 2 [51, 54, 55]	547.0	816.6	68.5	0.576	1.3E-11	2.4E-10	68.8
Erythromycin							
			See table 7 and 8				608 [46]

Table 2 CO_2-solute Peng-Robinson interaction parameters, determined by fitting the experimental data

T	k_{ij}	Caffeine		Uracil		Erythromycin
[ºC]		Set 1	Set 2	Set 1	Set 2	
40	CO_2	-0.060	-0.435	-0.184	-0.456	See Tables 7 & 8
60	CO_2			-0.266	-0.565	

Table 3 Solubility measurements of caffeine in SC CO_2 that have been published previously

Authors	Temperatures [ºC]	Pressure Range [bar]
Stahl and Shilz [20]	21,35,40,60	10-200
Gährs [21]	40,50,60,70,80	160-400
McHugh and Krukonis [47]	60	152-228
Lentz et al. [48]	36.9-156.9	150- 700
Saldaña et al. [17]	40, 60, 65, 70	140-240
Ebeling and Franck [49]	50-160	5-250
Johansen and Brunner [16]	39.9,59.9, 79.9	200-350
Li et al. [15]	40, 60, 80, 95	80-300

Table 4 Experimental solubility of caffeine in SC CO_2 at 40 ºC

Pressure [bar]	Density [g/cc]	Solubility [M]	Solubility [mole fraction]
100.0	0.6286	9.0E-04	6.3E-05
103.4	0.6513	1.2E-03	7.8E-05
137.9	0.7593	2.3E-03	1.4E-04
150.0	0.7802	2.6E-03	1.5E-04
172.4	0.8107	3.5E-03	1.9E-04
206.8	0.8460	4.8E-03	2.5E-04
300.0	0.9099	7.1E-03	3.7E-04

Table 5 Experimental solubility of uracil in SC CO_2 at 40 ºC and 60 ºC

Temperature [ºC]	Pressure [bar]	Density [g/cc]	Solubility [M]	Exp. Solubility [mole fraction]
40.1	100.0	0.6266	4.2E-05	2.9E-06
40.0	125.0	0.7311	4.9E-05	2.9E-06
40.2	150.0	0.7788	1.5E-04	8.4E-06
40.1	200.0	0.8392	2.3E-04	1.2E-05
40.1	249.9	0.8792	4.0E-04	2.0E-05
40.0	299.8	0.9100	7.4E-04	3.6E-05
60.1	100.0	0.2894	1.5E-05	2.3E-06
60.0	125.0	0.4717	2.7E-05	2.5E-06
60.0	150.0	0.6041	7.5E-05	5.5E-06
60.2	200.1	0.7225	4.4E-04	2.7E-05
60.1	250.0	0.7859	1.0E-03	5.8E-05
60.0	299.9	0.8295	2.4E-03	1.3E-04

Table 6 Experimental solubility of erythromycin in SC CO_2 at 40 ºC and 60 ºC

Temperature [ºC]	Pressure [bar]	Density [g/cc]	Solubility [M]	Exp. Solubility [mole fraction]
40.0	100.0	0.6286	Below detection	
40.0	150.0	0.7799	6.6E-03	3.8E-04
40.1	200.1	0.8396	1.7E-02	8.8E-04
40.2	249.9	0.8787	1.7E-02	8.8E-04
40.0	299.9	0.9097	1.8E-02	8.9E-04
60.0	100.0		Below detection	
60.0	150.0	0.6041	1.9E-02	1.4E-03
60.1	200.0	0.7233	2.8E-02	1.8E-03
60.1	249.9	0.7860	3.2E-02	1.8E-03
60.2	300.0	0.8290	3.8E-02	2.1E-03

Table 7 Estimated physical properties for erythromycin using various techniques

					Method used to estimate			
SET #	**T_b [K]**	**T_c [K]**	**P_c [bar]**	**ω**	**T_b**	**T_c**	**P_c**	**References**
1	1781.4	3033.9	6.5	-0.510	Joback	Joback	Joback	ASPEN Properties™
2	926.2	1577.3	6.5	-0.510	Meissner	Joback	Joback	ASPEN Properties™
3	926.2	1051.5	6.5	1.5458	Meissner	Fedors	Joback	ASPEN Properties™
4	926.2	1076.6	7.9	1.348	Meissner	Ambrose	Ambrose	ASPEN Properties™
5	926.2	1051.5	7.9	1.818	Meissner	Fedors	Ambrose	ASPEN Properties™

Table 8 Erythromycin sublimation pressure, binary interaction parameters with CO_2 and %AARD at 40ºC and 60ºC

SET #	T = 40 ºC			T = 60 ºC		
	P^{sub} [bar]	k_{ij}	%AARD	P^{sub} [bar]	k_{ij}	%AARD
1	2.5E-69	-2.603	52.0	3.0E-63	-2.810	14.9
2	2.9E-22	-1.519	111.1	9.1E-20	-1.495	34.8
3	2.9E-22	-0.083	69.4	9.1E-20	-0.100	29.3
4	2.9E-22	-0.094	15.6	9.1E-20	-0.109	35.9
5	2.9E-22	-0.031	8.1	9.1E-20	-0.045	41.4

List of Figures